

See discussions, stats, and author profiles for this publication at: <https://www.researchgate.net/publication/231645876>

Synthesis and Photovoltaic Properties of Copolymers from Benzodithiophene and Thiazole

ARTICLE *in* THE JOURNAL OF PHYSICAL CHEMISTRY C · SEPTEMBER 2010

Impact Factor: 4.77 · DOI: 10.1021/jp1063885

CITATIONS

51

READS

58

8 AUTHORS, INCLUDING:



Miao Yang

University of Wisconsin–Madison

5 PUBLICATIONS 85 CITATIONS

[SEE PROFILE](#)



Bo Peng

Nanyang Technological University

226 PUBLICATIONS 4,179 CITATIONS

[SEE PROFILE](#)



Yingping Zou

Central South University

95 PUBLICATIONS 2,817 CITATIONS

[SEE PROFILE](#)



Chunyue Pan

Central South University

20 PUBLICATIONS 363 CITATIONS

[SEE PROFILE](#)

Synthesis and Photovoltaic Properties of Copolymers from Benzodithiophene and Thiazole

Miao Yang,^{†,||} Bo Peng,^{†,||} Bo Liu,[‡] Yingping Zou,^{*,†,‡} Kechao Zhou,[‡] Yuehui He,[‡] Chunyue Pan,[†] and Yongfang Li^{*,§}

College of Chemistry and Chemical Engineering, Central South University, Changsha 410083, China, State Key Laboratory for Powder Metallurgy, Central South University, Changsha 410083, China, and Beijing National Laboratory for Molecular Sciences, Key Laboratory of Organic Solids, Institute of Chemistry, Chinese Academy of Sciences, Beijing 100190, China

Received: July 10, 2010; Revised Manuscript Received: September 11, 2010

Two new D–A conjugated polymers containing a benzodithiophene donor unit and the acceptor unit of bithiazole (BTz) or thiazolothiazole (TzTz), **P1** and **P2**, were synthesized by Stille cross-coupling polymerization. The thermal, optical, and electrochemical properties were well investigated. Bulk heterojunction polymer solar cell devices based on an active layer of electron donor copolymers, **P1** and **P2**, blended with electron acceptor [6,6]-phenyl-C₇₁ butyric acid methyl ester (PC₇₁BM) in a weight ratio of 1:2 were explored; the external quantum efficiency (EQE) measurements showed a peak external quantum efficiency of 45% for **P1** and **P2**. The first result of the PSC device with **P2** and PC₇₁BM in a weight ratio of 1:2 gave an overall power conversion efficiency (PCE) of 2.6%, an open-circuit voltage of 0.77 V, a short-circuit current of 6.68 mA/cm², and a fill factor of 0.51, under the illumination of AM1.5, 100 mW/cm².

1. Introduction

Recently, polymer solar cells (PSCs) have generated broad interest due to their unique features such as easy fabrication, low cost, light weight, and flexibility.¹ Bulk heterojunction (BHJ) type PSCs are the most widely used device architecture, which can ensure maximum internal donor–acceptor (D–A) interfacial area for efficient charge separation.² In the past two years, great progress in BHJ PSCs has been witnessed;³ power conversion efficiency (PCE) is still a big challenge toward commercialization. To further improve the PCE, it is very important to develop p-type conjugated polymers with low band gap, high hole mobility, and a deep-lying HOMO energy level.⁴

The donor–acceptor (D–A) approach is the most efficient strategy for obtaining low band-gap polymers and modulating their electronic properties.⁵ Among these D–A polymers, the copolymers using benzothiadiazole or 4,7-di-2-thienyl-2,1,3-benzothiadiazole as the accepting units with fluorene or fluorene-like units as the donor unit show promising photovoltaic properties with PCE up to 5%.⁶ Very recently, the D–A copolymers based on the diketopyrrolopyrrole acceptor unit also attracted considerable attention from the science community.⁷ In parallel, benzodithiophene (BDT) based conjugated polymers have demonstrated exceptional photovoltaic properties as electron donors for PSCs.⁸ For instance, Yang and Yu et al. synthesized a family of BDT-based copolymers with optimized electronic and optical properties which led to PCEs as high as 7%.⁹ This year, Leclerc et al. reported a new BDT-based polymer (PBDDTPD) using thienopyrroldione as the new and interesting accepting building block, with low band gap and preferred energy level, therefore exhibiting high PCE up to 5.5%

using a large active area of 1 cm².¹⁰ Although the results show that these low band gap polymers with proper energy level are promising in photovoltaic applications, the performances of these copolymers are still lower than the theoretical PCE value deduced from the model.¹¹ The deviation not only indicates that the photovoltaic properties are determined by band gap and energy level but also some other characteristics such as mobility, solubility, and morphology, etc., are also very important for high-efficiency photovoltaics. Much attention has been paid to the morphology on the performance of PSCs.¹² Different solvents, thermal annealing, chemical structure modification, and processing with solvent additives have been identified experimentally as significant factors affecting the nanoscale morphology. Usually bicontinuous nanoscale morphology can lead to a relatively higher short-circuit current (J_{sc}), good fill factor (FF), and therefore higher PCE than rough surfaces of the polymer films.¹³

Thiazole is a well-known electron-deficient unit because it contains one electron-withdrawing nitrogen of imine ($-C=N$) in place of the carbon atom at the 3-position of thiophene. Conjugated polymers bearing bithiazole (BTz) (two thiazole rings connected together) or thiazolothiazole (TzTz) (thiazole fused ring) moieties have demonstrated high mobilities for organic field effect transistors,¹⁴ and the PSCs from BTz- and TzTz-based D–A copolymers have shown high open-circuit voltage (V_{oc}), and a PCE close to 3% has been reported.¹⁵ These results indicate that BTz- or TzTz-based copolymers are probably promising photovoltaic donor materials. The BTz or TzTz unit seems a simple structure in comparison with other acceptor units such as dithienyl benzothiadiazole, etc. However, only a limited number of BTz- or TzTz-based copolymers have been explored for photovoltaic applications. Along these lines, the copolymers from BDT and bithiazole or thiazolothiazole probably possess interesting photovoltaic properties.

In this work, to shed light on the potential of BTz and TzTz as the electron-accepting unit, two new D–A conjugated copolymers containing a BDT donor unit and an acceptor unit

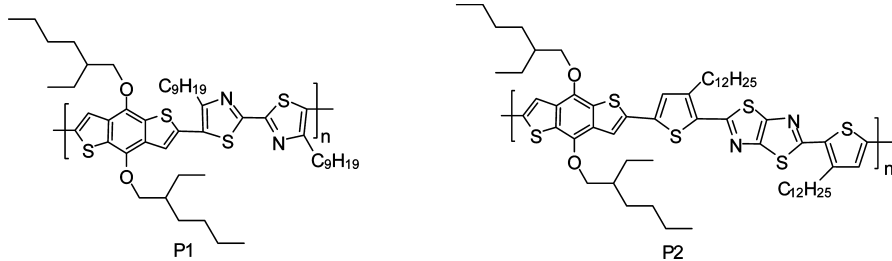
* To whom correspondence should be addressed. E-mail: zyp2008@iccas.ac.cn (Y. Zou).

[†] College of Chemistry and Chemical Engineering, Central South University.

[‡] State Key Laboratory for Powder Metallurgy, Central South University.

[§] Chinese Academy of Sciences.

^{||} M. Yang and B. Peng contributed equally to this work.

SCHEME 1: Molecular Structures of P1 and P2

of BTz or TzTz, **P1** and **P2** (as shown in Scheme 1), were designed and synthesized for photovoltaic applications. The copolymers were well characterized. The resulting copolymers/PC₇₁BM-blend films exhibited broad absorption spectra covering from 300 to ca. 700 nm. Compared to BDT homopolymer H2 ($\lambda_{\text{max}} = 495$ nm; $E_g^{\text{opt}} = 2.13$ eV),¹⁶ **P1** and **P2** showed the obvious red shift in the absorption maxima (ca. 530 nm) and the absorption edge of **P1** and **P2** is located at 620 and 638 nm, respectively, from their absorption spectra; therefore, the optical band gap of **P1** and **P2** is lower than that of the BDT homopolymer, which indicated that the D–A structure does reduce the band gap. In addition, **P1** film suggested high hole mobility up to 3.6×10^{-2} cm²/(V s) measured by the SCLC method. BHJ solar cells based on the blend of the polymers and PC₇₁BM showed that PCEs of **P2** and **P1** reached 2.6% and 2%, respectively, under the illumination of AM 1.5 G, 100 mW/cm². Moreover, the morphology effect on the photovoltaic properties is also investigated. Better nanoscale morphology can in part explain the higher PCE of than that of **P1** regardless of the lower hole mobility of **P2**. The above investigations indicate that the thiazole-based D–A copolymers will probably have great potential in organic electronics.

2. Experimental Section

2.1. Materials. Pd(PPh₃)₄, 2-undecanone, and dithiooxamide were obtained from Alfa Asia Chemical Co., 3-dodecylthiophene was obtained from Huicheng Chemical Co. Ltd., and 2,6-bis(trimethyltin)-4,8-di(2-ethylhexyloxy)benzo[1,2-*b*:3,4-*b*]dithiophene (**9**) was synthesized according to the literature.¹⁶ All other reagents and solvents were purchased commercially as analytical-grade quality and used without further purification.

2.2. Characterization. ¹H NMR spectra were recorded using a Bruker AV-400 spectrometer, with tetramethylsilane (TMS) as the internal reference; chemical shifts were recorded in ppm. Molecular weight and polydispersities of the copolymers were determined by gel permeation chromatography (GPC) analysis with polystyrene as the standard (Waters 515 HPLC pump, a Waters 2414 differential refractometer, and three Waters Styragel columns (HT2, HT3, and HT4)) using THF (HPLC grade) as the eluent at a flow rate of 1.0 mL/min at 35 °C. Thermogravimetric analysis (TGA) was conducted on a Shimadzu DTG-60 thermogravimetric analyzer with a heating rate of 10 K/min under a nitrogen atmosphere. The UV–vis absorption spectra were recorded on a JASCO V-570 spectrophotometer. For solid-state measurements, polymer films were obtained by drop casting on quartz plates from the chloroform solution. Optical band gap was calculated from the onset of the absorption band. The cyclic voltammogram was recorded with a computer-controlled Zahner IM6e electrochemical workstation (Germany) using polymer film on platinum disk as the working electrode, platinum wire as the counter electrode, and Ag/Ag⁺ (0.1M) as the reference electrode in an anhydrous and argon-saturated solution of 0.1 M tetrabutylammonium hexafluoro-

phosphate (Bu₄NPF₆) in acetonitrile. A trace amount of ferrocene (F_c) was used as a standard material to determine the molecular energy level of the polymers. Electrochemical onsets were determined at the position where the current starts to differ from the baseline. The morphology of the polymer/PCBM blend films was investigated by a SPI 3800N atomic force microscope (AFM) in contacting mode with a 1 μm scanner.

2.3. Device Fabrication and Characterization of Polymer Solar Cells.

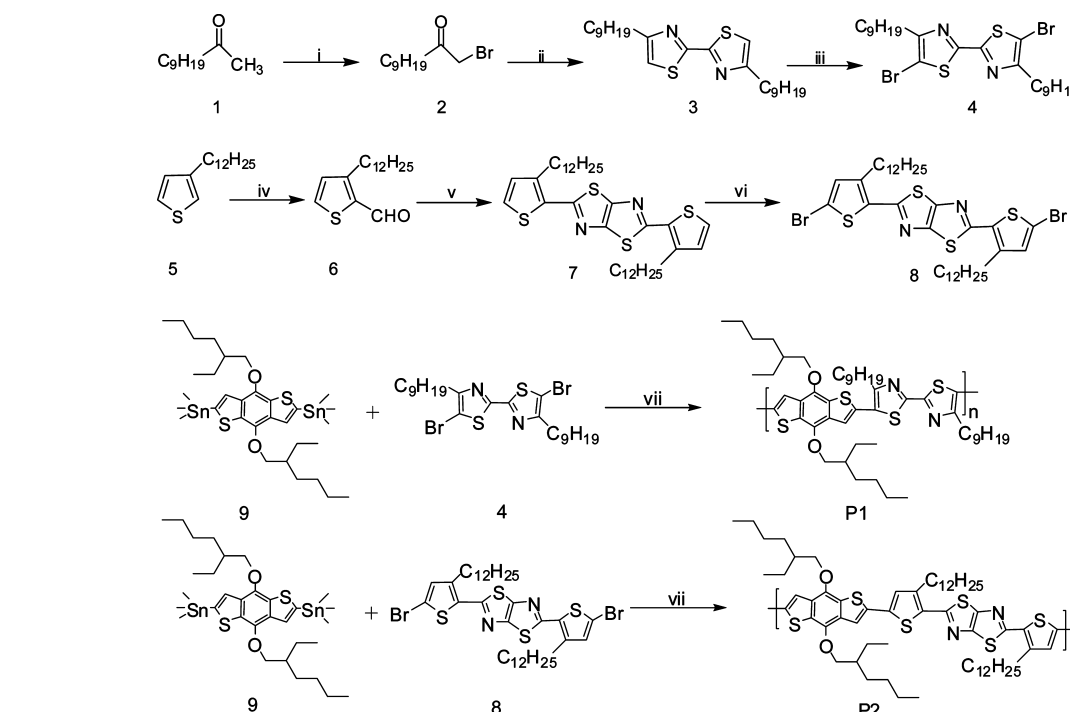
The polymer solar cells were fabricated in the configuration of the traditional sandwich structure with ITO glass as a positive electrode and Ca and Al as a metal negative electrode. Patterned ITO glass with a sheet resistance of 10 Ω/□ was purchased from CSG Holding Co., Ltd. (China). The ITO glass was cleaned by sequential ultrasonic treatment in detergent, deionized water, acetone, and isopropanol and then treated in an ultraviolet-ozone chamber (Ultraviolet Ozone Cleaner, Jelight Co., USA) for 20 min. A thin layer of poly(3,4-ethylenedioxythiophene):poly(styrene sulfonate) (PEDOT:PSS) (Baytron PVP AI 4083, Germany) was spin coated on the ITO glass and dried in a vacuum oven at 150 °C for 15 min. The thickness of the PEDOT:PSS layer was ca. 40 nm. Subsequently, the active layer was prepared by spin coating the *o*-dichlorobenzene solution of polymer:PC₇₁BM (1:2, w/w) with a polymer concentration of 12 mg mL⁻¹ on the top of the PEDOT:PSS layer, giving a thickness of ca. 80 nm determined by a surface profilometer (XP-2, USA). The devices were completed by evaporating Ca/Al metal electrodes defined by masks. The Ca electrode (10 nm) capped with Al (80 nm) was thermally deposited on the active layer at a pressure of 5×10^{-5} Pa. The active area of a device was 4 mm². The current intensity–voltage (*J*–*V*) measurement of the PSCs was conducted on a computer-controlled Keithley 236 source measure unit. A xenon lamp with an AM1.5 filter was used as a white-light source, and the optical power was 100 mW/cm². The EQE measurements of the PSCs were performed by a Stanford Research Systems model SR830 DSP lock-in amplifier coupled with a WDG3 monochromator and a 500 W xenon lamp. The light intensity at each wavelength was calibrated with a standard single-crystal Si photovoltaic cell. All measurements were automatically controlled by a computer system and performed under ambient atmosphere at room temperature.

2.4. Synthesis. All compounds and polymers were synthesized and characterized as shown in the Supporting Information.

3. Results and Discussion

3.1. Synthesis and Characterization. The general syntheses of the monomers and copolymers are outlined in Scheme 2, and synthetic details can be found in the Supporting Information. Compounds **4**,¹⁷ **8**,¹⁸ and **9**¹⁶ were prepared according to known literature procedures. Compound **9** copolymerized with compound **4** or **8** through Stille coupling reactions to afford the target polymers **P1** or **P2**, respectively. The polymers were purified by sequential Soxhlet extraction with methanol, hexane,

SCHEME 2: Synthetic Routes of the Monomers and Polymers^a



^a Reagents and conditions: (i) Br₂, CH₃OH, -10 °C, then 0 °C, 1 h, room temperature, 1 h, and then H₂O, H₂SO₄, room temperature, 24 h, 81% yield; (ii) NH₂CSCSNH₂, C₂H₅OH, reflux, 6 h, 88% yield; (iii) NBS, CH₃COOH, DMF, 4 h, 92% yield; (iv) Mg, I₂, THF, DMF, reflux, 6 h, 61% yield; (v) NH₂CSCSNH₂, 200 °C, 5 h, 27% yield; (vi) NBS, CHCl₃, reflux, 3 h, 70% yield; (vii) Pd(PPh₃)₄, toluene, reflux, 48 h.

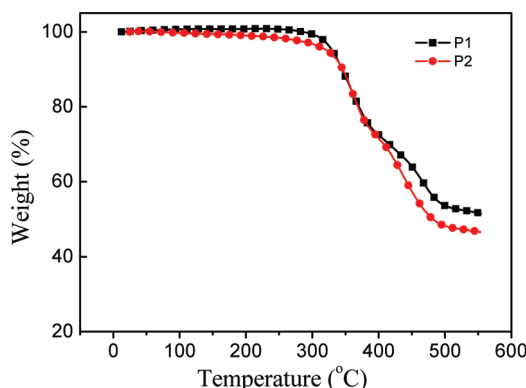


Figure 1. TGA plots of **P1** and **P2** with a heating rate of 10 °C/min in the air.

and CHCl_3 . The CHCl_3 fraction was then reduced in volume, precipitated into methanol, and collected by filtration, yielding a dark red solid. The chemical structures of the polymers were verified by ^1H NMR and elemental analysis. The molecular weight of the polymers was determined by gel-permeation chromatography (GPC) in tetrahydrofuran (THF) solution relative to polystyrene standards. The number-average molecular weight (M_n) of **P1** and **P2** is 6963 and 11 020, with a PDI of 1.4 and 1.3, respectively. The thermal properties of the polymers were investigated with thermogravimetric analysis (TGA), as shown in Figure 1. The two polymers exhibited similar thermal stability. TGA analysis displays that the 5% weight-loss temperatures (T_d) of **P1** and **P2** were found to be 330 and 322 °C in air, respectively, mainly due to removal of the alkoxy or alkyl groups. This indicates that the thermal stability of the copolymers is good for optoelectronic applications.

3.2. Optical Properties. The photophysical characteristics of the copolymers were investigated by UV-vis absorption spectra in diluted chloroform solutions and in the pure and blend

TABLE 1: Optical and Electrochemical Properties of the Synthesized Conjugated Copolymers

polymers	absorption spectra			cyclic voltammetry (vs Ag/Ag ⁺)		
	solution ^a		film ^b	<i>p</i> -doping		<i>n</i> -doping
	λ_{max} (nm)	λ_{max} (nm)	λ_{onset} (nm)	E_g^{opt} (eV) ^c	$E_{\text{on}}^{\text{ox}}$ / HOMO (V/eV) ^d	LUMO (eV) ^e
P1	490	530	620	2.0	0.33/-5.04	-3.04
P2	528	532	638	1.94	0.34/-5.05	-3.11

^a Measured in chloroform solution. ^b Cast from chloroform solution. ^c Band gap estimated from the onset wavelength of the optical absorption. ^d HOMO = -e(E_{on}^{ox} + 4.71) (eV). ^e LUMO = E^{opt} + HOMO.

films. Optical data are summarized in Table 1. The UV-vis absorption spectra of **P1** and **P2** in chloroform solutions are shown in Figure 2a. The absorption spectra of **P1** and **P2** in solution showed absorption maxima at 490 and 528 nm, respectively. The absorption spectra of **P1** and **P2** films and blends with PC₇₁BM are shown in Figure 2b. A similar absorption was observed in **P1** and **P2** films. The absorption of **P2** films exhibited well-defined vibronic splitting peaks at 530 and 575 nm, which reflects the high structural organization of the molecules in the **P2** film. **P1** seemly showing the shoulder peak at 570 nm. Generally, the polymers displayed strong absorption from 450 to 650 nm and the maximum absorption peak at around 530 nm in the film states. The absorption edge of **P1** and **P2** are at 620 and 638 nm, corresponding to the energy gap of 2.0 and 1.94 eV, respectively. In order to compensate for the absorption of **P1** and **P2** in the short wavelength region, PC₇₁BM is used as the electron acceptor, which have similar electronic structure with PC₆₀BM but stronger absorption from 300 to 530 nm.¹⁹ The resulting copolymers/PC₇₁BM-blend films exhibit a similar broad absorption covering the range from 300 to ca.700 nm, which is

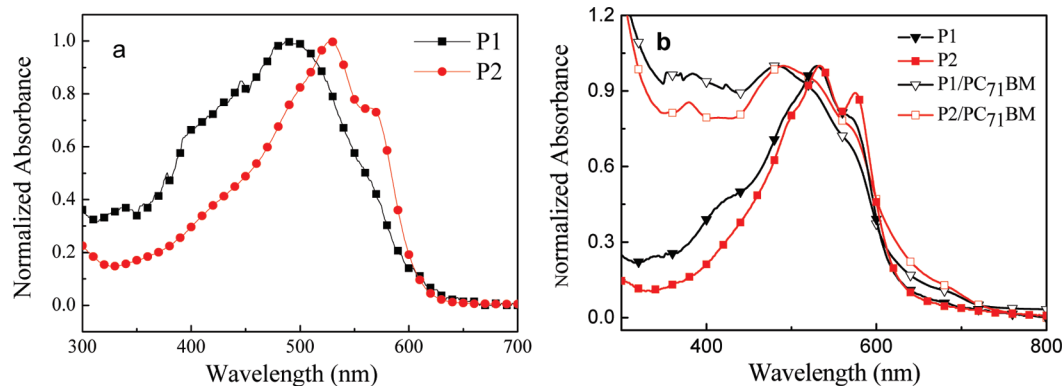


Figure 2. Absorption spectra of the copolymers (a) solution in chloroform; (b) copolymers in the film states and blend films of copolymers/PC₇₁BM in a 1:2 weight ratio.

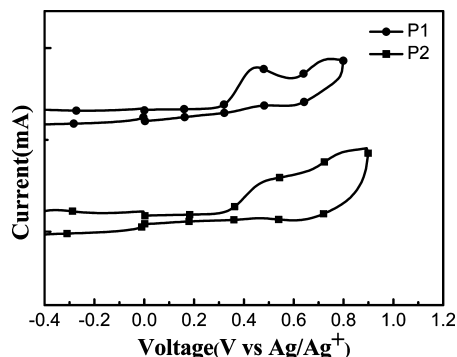


Figure 3. Cyclic voltammograms of **P1** and **P2** films on platinum electrode in 0.1 mol/L Bu₄NPF₆, CH₃CN solution.

beneficial for obtaining high-efficiency polymer solar cells from an absorption viewpoint. For the absorption of the blend films, the absorption peak blue shifted compared to that of the polymers, which is probably due to dilution of the PCBM in polymer films.

3.3. Electrochemical Properties. In order to investigate the electrochemical properties of **P1** and **P2** and estimate their highest occupied molecular orbital (HOMO) and lowest unoccupied molecular orbital (LUMO) energy levels, cyclic voltammetry (CV) was carried out in a 0.1 M solution of Bu₄NPF₆ in acetonitrile at room temperature under argon with a scanning rate of 50 mV/s. All potentials are reported vs Ag/Ag⁺ with the ferrocene/ferrocenium couple as an internal standard. CV curves of **P1** and **P2** are shown in Figure 3. The related electrochemical data are listed in Table 1. In a positive potential region, the oxidation is quasi-reversible; the onset oxidation potential ($E_{\text{on}}^{\text{ox}}$) is 0.33 V vs Ag/Ag⁺ for **P1**. For **P2**, $E_{\text{on}}^{\text{ox}}$ is 0.34 V vs Ag/Ag⁺. From $E_{\text{on}}^{\text{ox}}$ of the polymers, we calculated the HOMO and LUMO energy levels of the polymer according to the equations²⁰

$$E_{\text{HOMO}} = -e(E_{\text{on}}^{\text{ox}} + 4.71) \text{ (eV)}$$

E_{LUMO} was from E_g^{opt} and E_{HOMO} . The E_{LUMO} and E_{HOMO} values of **P1** are -3.04 and -5.04 eV, respectively. The E_{LUMO} and E_{HOMO} values of **P2** are -3.11 and -5.05 eV, respectively. The HOMO level of **P1** is very similar to that of **P2**. The electrochemical results show that the two copolymers exhibit a similar energy level, although of a different chemical structure. Compared to the high HOMO level of P3HT (-4.76 eV),²¹ the copolymers with a deep-lying HOMO energy level indicate that the electron-withdrawing thiazole unit into the polymer back-

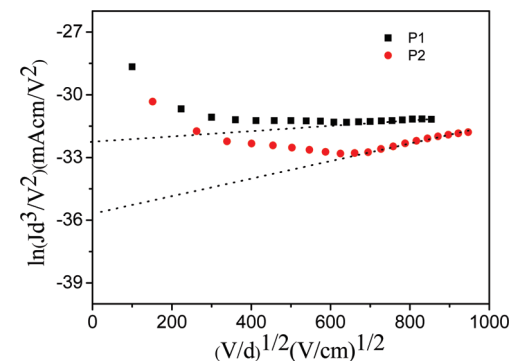


Figure 4. $\ln(Jd^3/V^2)$ vs $(V/d)^{1/2}$ plots of the polymers for measurement of hole mobility by the SCLC method.

bone is a good choice to lower the HOMO level and therefore result in the higher V_{oc} with PCBM as the acceptor.

3.4. Hole Mobility. Hole mobility is another important parameter of the conjugated polymers for photovoltaic applications. Here we investigated the hole mobility of **P1** and **P2** by the space-charge-limited current (SCLC) model with a device structure of ITO/PEDOT:PSS/polymer/Au.²² For the hole-only devices, SCLC is described by

$$J_{\text{SCLC}} = \frac{9}{8} \varepsilon_0 \mu_0 \frac{(V - V_{\text{bi}})^2}{d^3} \exp \left[0.89 \gamma \sqrt{\frac{V - V_{\text{bi}}}{d}} \right] \quad (1)$$

The results are plotted as $\ln(Jd^3/V^2)$ vs $(V/d)^{1/2}$, as shown in Figure 4, where J stands for current density, d is the thickness of the device, $V = V_{\text{appl}} - V_{\text{bi}}$, V_{appl} is the applied potential, and V_{bi} is the built-in potential. According to eq 1 and Figure 4, the hole mobilities are evaluated to be $3.6 \times 10^{-2} \text{ cm}^2/(\text{V s})$ and $9.8 \times 10^{-4} \text{ cm}^2/(\text{V s})$ for **P1** and **P2**, respectively. Obviously, the hole mobilities of **P1** and **P2** are relatively high as photovoltaic donor materials in PSCs.

3.5. Photovoltaic Properties. To explore the photovoltaic properties of the two copolymers, BHJ PSC devices with a structure of ITO/PEDOT:PSS/Polymer:PC₇₁BM (1:2 w/w)/Ca/Al were fabricated. The polymer active layers were spin-coated from a dichlorobenzene solution. Figure 5 shows typical current density–voltage ($J-V$) curves and the external quantum efficiency (EQE) of the PSCs. The corresponding open-circuit voltage (V_{oc}), short-circuit current (J_{sc}), fill factor (FF), and power conversion efficiency (PCE) of the devices are summarized in Table 2. Both J_{sc} and V_{oc} are very close for **P1**- and **P2**-based solar cells to each other; the high J_{sc} comes from strong

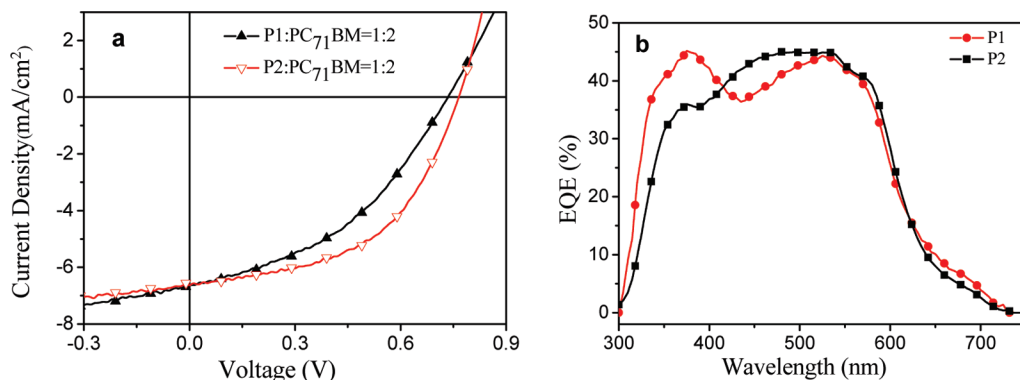


Figure 5. (a) J - V curves of the PSCs based on **P1** and **P2**:PC₇₁BM (1:2, w/w), under illumination of AM 1.5, 100 mW/cm². (b) EQE of PSCs based on **P1** and **P2**:PC₇₁BM (1:2, w/w).

TABLE 2: Photovoltaic Performances of the Polymer Solar Cells Based on P1 and P2

polymer/PC ₇₁ BM(1:2)	V_{oc} (V)	J_{sc} (mA/cm ²)	FF (%)	PCE (%)
P1	0.73	6.63	42	2.03
P2	0.77	6.68	51	2.60

absorbance and good charge transport in the active layer. The relatively higher V_{oc} is from the deep-lying HOMO level compared to that of P3HT. PCE of **P2** reached 2.6%, which is better than that of **P1** (2%). The difference of PCEs is clearly from the different FF of the polymers as shown in J - V curves.

Figure 5b shows the EQE of the PSC devices with **P1** and **P2**:PC₇₁BM by a weight ratio of 1:2. Comparing the EQE of devices with the absorption spectra of **P1** and **P2** films, the contribution from PC₇₁BM to the photocurrent is very pronounced. The device of **P1** demonstrated a relatively high photoconversion efficiency over the broad plateau of 340–600 nm, with monochromatic EQE values above 30%; the maximum EQE value of 45% is at 530 nm. For **P2**, a broad EQE plateau of 45% covers from 430 to 550 nm. High and broad EQE values in part reflect the high J_{sc} of the copolymers.

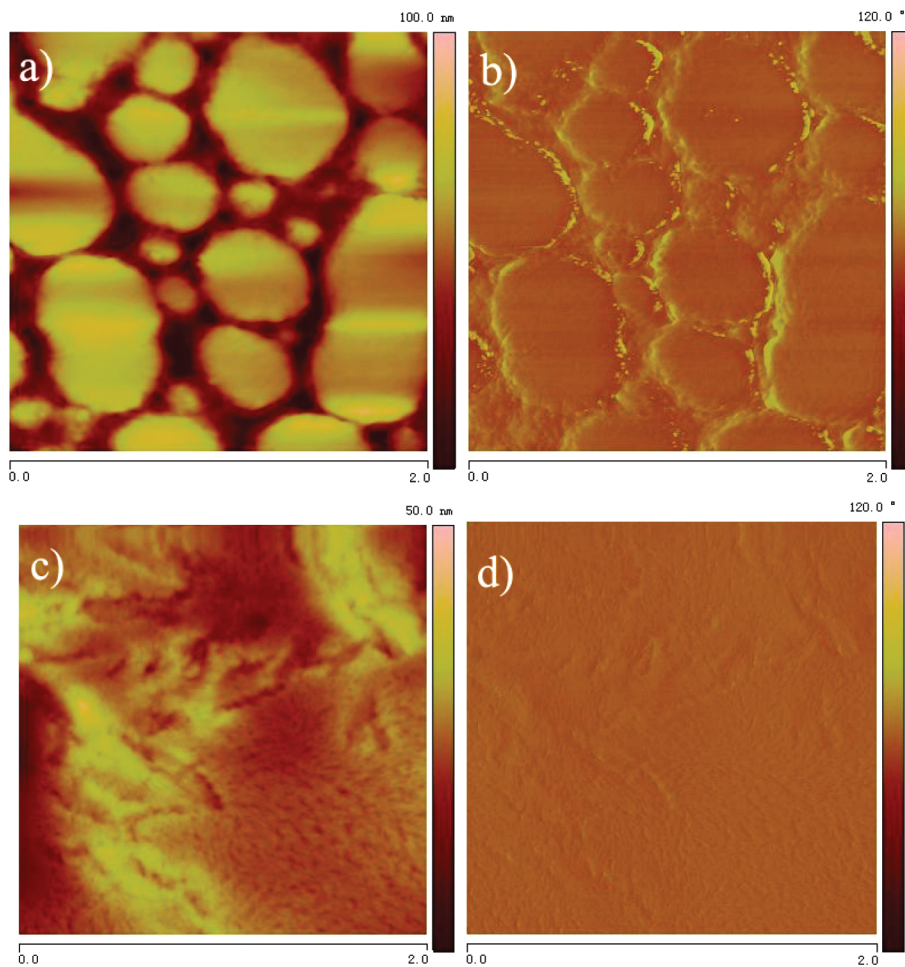


Figure 6. AFM (2 μ m \times 2 μ m) topography (a and c) and phase images (b and d) for polymer:PC₇₁BM blend films (1:2, w/w): (a and b) **P1**; (c and d) **P2**.

3.6. Morphology. The morphology of the photoactive layer is very important for the performance of PSCs, and in some cases the performance of the device strongly depends on its morphological features.²³ To investigate in more detail the reasons for the higher performance of **P2**, although **P1** possesses higher hole mobility than **P2**, we used atomic force microscopy (AFM) to investigate the surface morphology of the copolymer: PC₇₁BM (1:2, w/w) blend films by spin coating the *o*-dichlorobenzene solution of the blend. The AFM topography and phase images are shown in Figure 6. The surface rms (root-mean-square) roughness of the polymer:PC₇₁BM films (1:2, w/w) are 19.47 and 3.31 nm for **P1** and **P2**, respectively. For **P1**/PC₇₁BM blend, Figure 6a reveals that the domains are not well distributed throughout the surface, indicating a significant aggregation of one component (**P1** or PC₇₁BM) as shown in Figure 6b, which probably influences the separation of charges; therefore, an unbalanced charge transporting property was produced. For **P2**/PC₇₁BM blend, the blend films are smoother (rms 3.31 nm) than that of **P1**/PC₇₁BM (rms 19.47 nm); in addition, from the phase image (Figure 6d), there is an absence of large-scale accumulation of **P2** or PC₇₁BM; the polymer **P2** and PC₇₁BM domains are homogenously distributed throughout the surface of the film, suggesting that **P2** was highly compatible with PC₇₁BM. In other words, **P2** possesses higher photovoltaic properties than **P1** regardless of the higher hole mobility of **P1**, which is probably due to the smoother, more homogeneous morphology and better nanoscale interpenetrating network in the **P2**/PC₇₁BM blend.²⁴ The rough surface, big domains, and coarse phase separation of the **P1**/PC₇₁BM, at least in part, explain the relatively lower PCE; however, **P1** still holds potential to improve the photovoltaic property by modifying the morphology using optimal methods. The results confirm further that the design of the low band gap polymers for photovoltaic applications should consider not only lowering the gap but also improving charge transport as well as the favorable morphology of the blend films.

4. Conclusion

In summary, we synthesized two new D–A conjugated polymers containing a BDT donor unit and an acceptor unit of BTz or TzTz, **P1** and **P2**, by Stille cross-coupling polymerization reactions. The synthesized copolymers exhibited good absorption in the visible region and high hole mobility. Preliminary studies on photovoltaic cells using the blends of **P2** and PC₇₁BM (1:2, w/w) as the active layer afforded devices with a *V*_{oc} of 0.77 V, *FF* of 0.51, and PCE of 2.6%. For **P1** with a similar device structure, the PCE of **P1** reached 2%. The first photovoltaic results of these two copolymers clearly demonstrate that BTz and TzTz are promising electron-accepting units for constructing D–A copolymers. A higher PCE can be anticipated by careful device engineering such as a different blend ratio, additive and thermal annealing, etc.

Acknowledgment. This work was supported by the National Natural Science Foundation of China (nos. 50803074, 50825102, 50633050, 20976199), Lieying Project, Fundamental Research Funds for the Central Universities, and Opening Fund of State Key Laboratory of Powder Metallurgy.

Supporting Information Available: Synthesis of the monomers and polymers. This material is available free of charge via the Internet at <http://pubs.acs.org>.

References and Notes

- (a) Heeger, A. J. *Chem. Soc. Rev.* **2010**, *39*, 2354. (b) Cheng, Y. J.; Yang, S. H.; Hsu, C. S. *Chem. Rev.* **2009**, *11*, 5868. (c) Shen, P.; Sang, G.; Lu, J.; Zhao, B.; Wan, M. X.; Zou, Y.; Li, Y.; Tan, S. *Macromolecules* **2009**, *41*, 5716.
- (2) Yu, G.; Gao, J.; Hummelen, J. C.; Wudl, F.; Heeger, A. J. *Science* **1995**, *270*, 1789.
- (3) (a) Chen, J. W.; Cao, Y. *Acc. Chem. Res.* **2009**, *11*, 1709. (b) Zhan, X. W.; Zhu, D. B. *Polym. Chem.* **2010**, *1*, 409.
- (4) Li, Y.; Zou, Y. *Adv. Mater.* **2008**, *20*, 2952.
- (5) Zhang, Z. H.; Peng, B.; Liu, B.; Pan, C. Y.; Li, Y. F.; He, Y. H.; Zhou, K. C.; Zou, Y. *Polym. Chem.* **2010**, DOI: 10.1039/c0py00136h. (b) Yue, W.; Zhao, Y.; Shao, S. Y.; Tian, H. K.; Xie, Z. Y.; Geng, Y. H.; Wang, F. S. *J. Mater. Chem.* **2009**, *19*, 2199.
- (6) (a) Hou, J. H.; Chen, H. Y.; Zhang, S.; Li, G.; Yang, Y. *J. Am. Chem. Soc.* **2008**, *130*, 16144. (b) Wang, E. G.; Wang, L.; Lan, L. F.; Luo, C.; Zhuang, W. L.; Peng, J. B.; Cao, Y. *Appl. Phys. Lett.* **2008**, *92*, 033307.
- (7) (a) Zou, Y. P.; Gendron, D.; Aïch, R. B.; Najari, A.; Tao, Y.; Leclerc, M. *Macromolecules* **2009**, *42*, 2891. (b) Zou, Y.; Gendron, D.; Neagu-Plesu, R.; Leclerc, M. *Macromolecules* **2009**, *42*, 6361.
- (8) Hou, J.; Chen, H.; Zhang, S.; Chen, R.; Yang, Y.; Wu, Y.; Li, G. *J. Am. Chem. Soc.* **2009**, *131*, 15586.
- (9) Chen, H.; Hou, J.; Zhang, S.; Liang, Y.; Yang, G.; Yang, Y.; Yu, L.; Wu, Y.; Li, G. *Nat. Photonics* **2009**, *3*, 649.
- (10) Zou, Y.; Najari, A.; Berrouard, P.; Beaupré, S.; Aïch, R. B.; Tao, Y.; Leclerc, M. *J. Am. Chem. Soc.* **2010**, *132*, 5330.
- (11) Scharber, M. C.; Mühlbacher, D.; Koppe, M.; Denk, P.; Waldauf, C.; Heeger, A. J.; Brabec, C. J. *Adv. Mater.* **2006**, *18*, 789.
- (12) Peet, J.; Heeger, A. J.; Bazan, G. C. *Acc. Chem. Res.* **2009**, *11*, 1700.
- (13) Hoven, C. V.; Dang, X. D.; Coffin, R. C.; Peet, J.; Nguyen, T. Q.; Bazan, G. C. *Adv. Mater.* **2010**, *22*, E63.
- (14) (a) Politis, J. K.; Curtis, M. D.; Gonzalez, L.; Martin, D. C.; He, Y.; Kanicki, J. *Chem. Mater.* **1998**, *10*, 1713. (b) Mamada, M.; Nishida, J. I.; Kumaki, D.; Tokito, S.; Yamashita, Y. *Chem. Mater.* **2007**, *19*, 5404. (c) Osaka, I.; Zhang, R.; Liu, J.; Smilgies, D.; Kowalewski, T.; McCullough, R. D. *Chem. Mater.* **2010**, *22*, 4191.
- (15) Li, K. C.; Huang, J. H.; Hsu, Y. C.; Huang, P. J.; Chu, C. W.; Lin, J. T.; Ho, K. C.; Wei, K. H.; Lin, H. C. *Macromolecules* **2009**, *42*, 3681.
- (16) Hou, J.; Park, M. H.; Zhang, S.; Yao, Y.; Chen, L. M.; Li, J. H.; Yang, Y. *Macromolecules* **2008**, *41*, 6012.
- (17) Wong, W. Y.; Wang, X. Z.; He, Z.; Chan, K. K.; Djurisic, A. B.; Cheung, K. Y.; Yip, C. T.; Ng, A. M. C.; Xi, Y. Y.; Mak, C. S. K.; Chan, W. K. *J. Am. Chem. Soc.* **2007**, *129*, 14372.
- (18) Osaka, I.; Sauve, G.; Zhang, R.; Kowalewski, T.; McCullough, R. D. *Adv. Mater.* **2007**, *19*, 4160.
- (19) Wienk, M. M.; Kroon, J. M.; Verhees, W. J. H.; Knol, J.; Hummelen, J. C.; van Hal, P. A.; Janssen, R. A. J. *Angew. Chem., Int. Ed.* **2003**, *42*, 3371.
- (20) Sun, Q. J.; Wang, H. Q.; Yang, C. H.; Li, Y. F. *J. Mater. Chem.* **2003**, *13*, 800.
- (21) Hou, J. H.; Tan, Z. A.; Yan, Y.; He, Y. J.; Yang, C. H.; Li, Y. F. *J. Am. Chem. Soc.* **2006**, *128*, 4911.
- (22) (a) Malliaras, G. G.; Salem, J. R.; Brock, P. J.; Scott, C. *Phys. Rev. B* **1998**, *58*, 13411. (b) Martens, H. C. F.; Brom, H. B.; Blom, P. W. M. *Phys. Rev. B* **1999**, *60*, 8489. (c) Yang, C. H.; Hou, J. H.; Zhang, B.; Zhang, S. Q.; He, C.; Fang, H.; Ding, Y. Q.; Ye, J. P.; Li, Y. F. *Macromol. Chem. Phys.* **2005**, *206*, 1311. (d) Roman, L. S.; Inganás, O. *Synth. Met.* **2002**, *125*, 419.
- (23) Qin, R.; Li, W.; Li, C.; Du, C.; Veit, C.; Schleiermacher, H.; Andersson, M.; Bo, Z.; Liu, Z.; Inganás, O.; Wuerfel, U.; Zhang, F. *J. Am. Chem. Soc.* **2009**, *131*, 14612.
- (24) Kim, M. S.; Kim, B. G.; Kim, J. *ACS Appl. Mater. Interfaces* **2009**, *1*, 1264.